Received: 24 June 2022 | Revised: 16 September 2022 | Accepted: 6 October 2022

DOI: 10.1111/cas.15636

Cancer Science WILEY

ORIGINAL ARTICLE

# Feedforward loop between IMP1 and YAP/TAZ promotes tumorigenesis and malignant progression in glioblastoma

Jia Yang[1,2] | Xujia Wu[1,2] | Jia Wang[3] | Xing Guo[4] | Junju Chen[1,2] | Xuesong Yang[1,2] | Jian Zhong[1,2] | Xixi Li[1,2] | Zhong Deng[1,2]

[1]Department of Neurosurgery, The First Affiliated Hospital of Sun Yat-sen University, Guangzhou, China

[2]Guangdong Provincial Key Laboratory of Brain Function and Disease, Guangdong Translational Medicine Innovation Platform, Guangzhou, China

[3]Department of Neurosurgery, The First Affiliated Hospital of Xi'an Jiaotong University, Xi'an, China

[4]Department of Neurosurgery, Qilu Hospital, Cheeloo College of Medicine and Institute of Brain and Brain-Inspired Science, Shandong University, Jinan, Shandong, China

**Correspondence**
Zhong Deng, Department of Neurosurgery, Guangdong Provincial Key Laboratory of Brain Function and Disease, The First Affiliated Hospital of Sun Yat-sen University, No58 Zhongshan 2 Road, Guangzhou, Guangdong 510080, China.
Email: dz8981201@126.com

## Abstract

YAP/TAZ have been identified as master regulators in malignant phenotypes of glioblastoma (GBM); however, YAP/TAZ transcriptional disruptor in GBM treatment remains ineffective. Whether post-transcriptional dysregulation of YAP/TAZ improves GBM outcome is currently unknown. Here, we report that insulin-like growth factor 2 (IGF2) mRNA-binding protein 1 (IGF2BP1 or IMP1) is upregulated in mesenchymal GBM compared with proneural GBM and correlates with worse patient outcome. Overexpression of IMP1 in proneural glioma stem-like cells (GSCs) promotes while IMP1 knockdown in mesenchymal GSCs attenuates tumorigenesis and mesenchymal signatures. IMP1 binds to and stabilizes m6A-YAP mRNA, leading to activation of YAP/TAZ signaling, depending on its m6A recognition and binding domain. On the other hand, TAZ functions as enhancer for IMP1 expression. Collectively, our data reveal a feedforward loop between IMP1 and YAP/TAZ maintaining GBM/GSC tumorigenesis and malignant progression and a promising molecular target in GBM.

**KEYWORDS**
glioblastoma, IMP1, malignant progression, YAP/TAZ pathway

## 1 | INTRODUCTION

Glioblastoma (GBM) is the most devastating primary brain tumor with only 7.2% of patients surviving longer than 5 years.[1] Genomic analysis of GBM has yielded a gene expression–based molecular classification and identified three different signatures termed proneural (PN), classical (CL), and mesenchymal (Mes),[2-4] and the mesenchymal subtype is considered the most malignant one correlating with worse outcome and treatment resistance.[2,5] To date, the molecular classification has been still suitable to define cancer cell states on the single-cell level.[6,7] Despite cellular and genetic diversity in GBM, tumor cell states could be influenced by microenvironmental and therapeutic stimuli and exhibit plasticity. Malignant progression to mesenchymal signature is a commonly occurring process and could be induced by multiple factors, such as hypoxia, VEGF and radiation, and interactions between cancer cells and immune cells.[2,7,8,9,10,11,12]

YAP and TAZ, two cotranscriptional regulators in the hippo signaling pathway, are highly activated in human malignancy.[13,14] The upstream regulators of YAP/TAZ are LATS1/2, while downstream gene transcription is mediated through YAP/TAZ binding to the TEAD family transcription factors (TEAD1-4).[13,15] YAP/TAZ are highly activated and correlate with reduced survival in GBM[16,17] and also function as key regulators in malignant phenotypes including stemness, radioresistance, and glucose addiction.[18-20] Noteworthy, TAZ is identified as one of the master regulators in mesenchymal GBM,[16,21] and overexpression of TAZ promotes mesenchymal-like transition and correlates

Jia Yang, Xujia Wu, and Jia Wang contributed equally.

with aggressive tumors in mouse model,[16] suggesting great therapeutic potential in GBM.[22] However, verteporfin, the only FDA-approved YAP/TAZ-TEAD interaction inhibitor, fails to show treatment efficacy because of low blood-brain barrier penetration. Modified form of verteporfin and other hippo pathway inhibitors are under investigation in the treatment of GBM and other malignancy.[15,22]

Insulin-like growth factor 2 (IGF2) mRNA-binding protein 1 (IGF2BP1, also named IMP1) is a single-strand RNA-binding protein, composed of two RNA recognition motif (RRM) domains and four type I K homology (KH) domains.[23] IMP1 is identified as an $m^6A$ readers and promotes $m^6A$-modified mRNAs' stability and translation.[24] In multiple malignancy, IMP1 promotes cancer malignant characteristics, including cancer stem cell maintenance, tumor growth, and metastasis.[25,26] Little is known about the physiological role of IMP1 in GBM. In the present study, we identified for the first time IMP1 as one of the highly expressed RNA binding proteins (RBPs) in Mes GBM and glioma stem-like cells (GSCs). Further investigation proved that IMP1 forms a feedforward loop with YAP/TAZ and hence promotes GBM/GSC tumorigenesis and malignant progression.

## 2 | MATERIALS AND METHODS

### 2.1 | Human tissues, animal care and ethics

A total of 123 pathologically diagnosed glioma samples ($n = 110$) and nontumor tissue from resected brain epileptic tissues ($n = 13$) were collected from the First Affiliated Hospital of Xi'an Jiaotong University, and eight paired tumor and adjacent nontumor tissues were collected from the First Affiliated Hospital of Sun Yat-sen University, with written informed consent, respectively. The study was approved by the Clinical Research Ethics Committee with the approval No. 2021-172. Four- to six-week-old female BALB/c-nu mice were purchased from the Laboratory Animal Center of Sun Yat-sen University. All animal procedures were reviewed and approved by the Institutional Animal Care and Use Committee (IACUC) at Sun Yat-sen University in accordance with NIH and institutional guidelines, conforming to the provisions of the Declaration of Helsinki.

### 2.2 | Actinomycin Dassay

Glioma stem-like cells were equally seeded ($5\times10^4$ cells per well) for at least 12 hours prior to actinomycin D treatment. After 2 μg/ml actinomycin D (HY-17559, MedChem Express) treatment at the indicated time points (0, 2, 4, 6, and 8 hours), the cells were harvested for RNA isolation. The relative YAP mRNA was analyzed by RT-PCR and normalized to the values measured in the 0 h group.

### 2.3 | ChIP-PCR assay

Chromatin immunoprecipitation (ChIP) assays were performed using a One Step ChIP Kit (Abcam, #ab117138) according to the manufacturer's instructions. Cell lysates were incubated with 2 μg of anti-FLAG antibody (#F1804, 1:1000, Sigma-Aldrich), mouse IgG, and anti-RNA polymerase II (#ab264350, Abcam, used as positive control). The resultant DNA was subjected to Northern blotting for further analysis. Primers are listed in Table S1.

### 2.4 | RNA immunoprecipitation (RIP)

RNA RIP was performed as previously described.[27] Briefly, after washing with ice-cold PBS, $1\times10^7$, cells were resuspended in 400 μl ice-cold PEB buffer (20 mM Tris HCl, pH 7.5, 100 mM KCl, 5 mM MgCl2, RNase inhibitor, and protein inhibitor) and incubated for 10 minutes on ice. Then, 1000 μg of precleared protein lysate was incubated with 50 μl of IMP1 antibody (#22803-1-AP, Proteintech) or FLAG antibody (F1804, Sigma-Aldrich) cross-linked protein A agarose beads for 1 hour at 4°C. Immunoprecipitated RBP-RNA complexes were washed five times with ice-cold NT2 buffer (50 mM Tris HCl, pH 7.5, 150 mM NaCl, 1 mM MgCl2, 0.05% Nonidet P-40). Coprecipitated RNAs were recovered with Trizol-chloroform and analyzed simultaneously by RT-PCR.

### 2.5 | Xenograft models

Glioma stem-like cells were implanted intracranially using a stereotactic instrument in 4- to 6-week-old female Nu/nu mice. Each mouse was randomly assigned and injected with 50,000 GSC cells in 5 μl PBS according to the experiment design. A minimum of six mice were used in each group. Mice were sacrificed at indicated time points, and brains were fixed in formalin and subjected to H&E and immunohistochemistry (IHC) staining. For the survival analysis, mice were monitored until they developed neurologic symptoms such as seizures, ataxia, lethargy, and inability to feed, or 100 days post implantation. The overall survival curves were calculated with the Kaplan-Meier method and compared by the log-rank test.

### 2.6 | Statistical analysis

Statistical tests were conducted using GraphPad Prism (Version 8) unless otherwise indicated. The data are presented as the mean ± standard deviation (SD) from three independent experiments. For the comparison of parametric data, two-tailed Student's *t* tests or one-way ANOVA were used. Survival curves were assessed with the Kaplan-Meier method and compared by the log-rank test. The cutoff values of IMP1 expression level in public datasets were analyzed by R reprogramming (version 4.1.0) with *survminer* package. The correlations between expression level of IMP1 and TAZ or YAP were calculated by Pearson correlation analysis. The statistical significance as *P* values is indicated in the figures: $^*p<0.05$; $^{**}p<0.001$; $^{***}p<0.0001$; ns, not significant. For all experiments, analyses were done in biological triplicates. No animals or data points were excluded from the analyses for any reason. Statistical analyses for the RNA-seq data are described in the respective sections.

## 3 | RESULTS

### 3.1 | IMP1 is upregulated in Mes GBM and correlates with worse survival

We first sought to examine IMP1 mRNA expression in public glioma datasets, such as TCGA, Chinese Glioma Genome Atlas (CGGA), Bao dataset, and Gill dataset, and found that IMP1 mRNA level was the highest in grade IV glioma compared with grade II and III glioma (Figure 1A). We further analyzed the expression of IMP1 mRNA among molecular subtypes of GBM and identified that IMP1 was more highly expressed in Mes GBM than in PN GBM, CL GBM, or nontumor (NT) tissue in multiple datasets (Figure 1B). Kaplan-Meier survival analysis demonstrated higher IMP1 mRNA level correlating

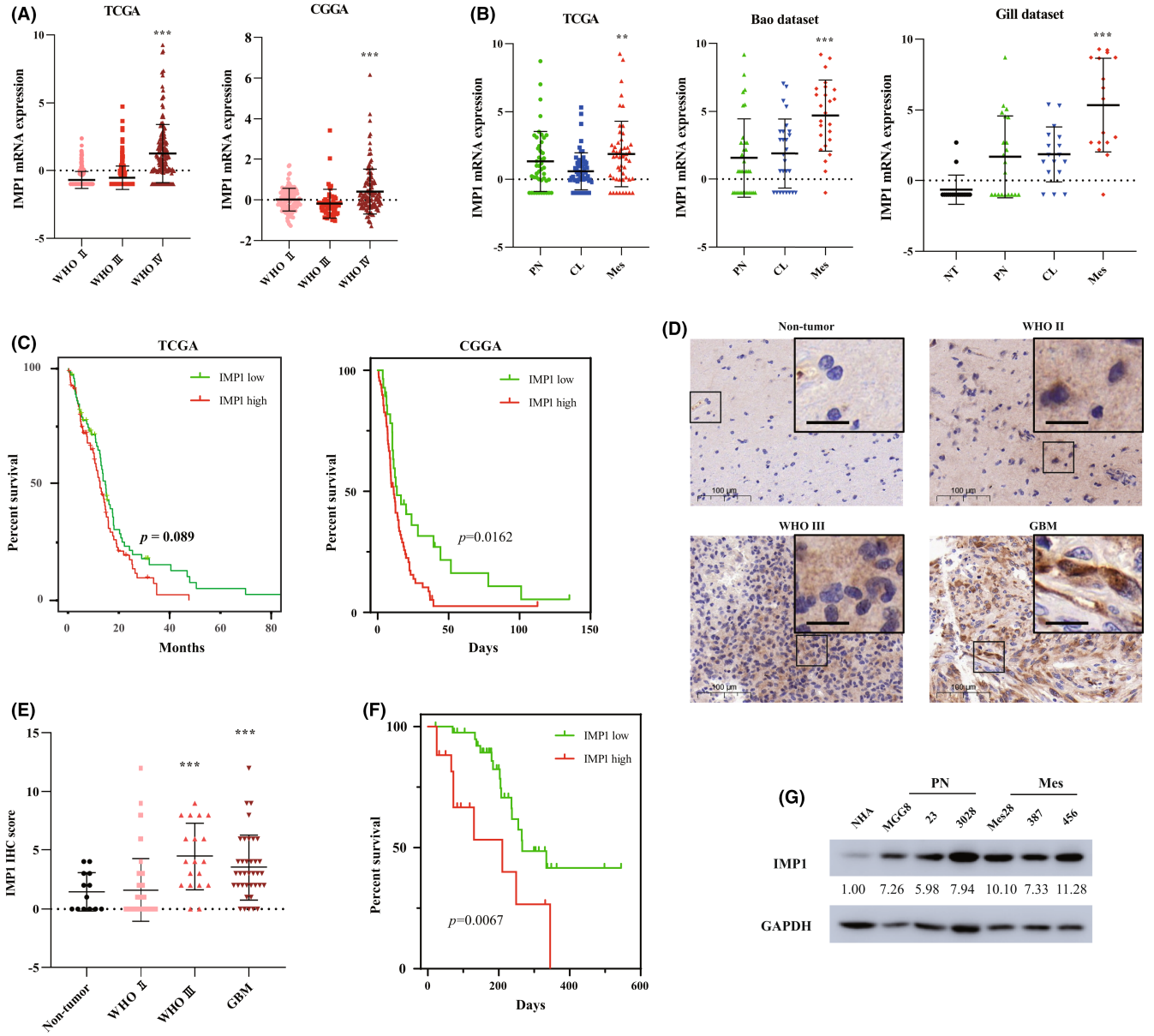


FIGURE 1 IMP1 is highly expressed in glioblastoma (GBM) and correlated with short overall survival. (A) Histograms of IMP1 mRNA expression among WHO II, III, and IV glioma across TCGA and CGGA dataset. Data represent mean ± SD (B) Histograms of IMP1 mRNA expression among GBM subtypes and nontumor tissues across TCGA, Bao dataset, and Gill dataset. Data represent mean ± SD (C) Kaplan-Meier survival curve of IMP1 high vs. IMP1 low in GBM patients from TCGA and CGGA datasets; the log-rank *P* value is $p = 0.089$, and $p = 0.0162$, respectively. (D) Representative immunohistochemistry (IHC) images for IMP1 expression in formalin-fixed paraffin-embedding (FFPE) human glioma tissues and nontumor tissues in our cohort of tissue bank. Scale bar represents 20 μm. (E) Histogram of IMP1 IHC score in nontumor tissues and glioma in our cohort of tissue bank. $n_{nontumor} = 13$, $n_{WHO\ II} = 54$, $n_{WHO\ III} = 19$, $n_{GBM} = 37$. Data represent mean ± SD. (F) Kaplan-Meier curve of IMP1 low (IHC score < 6, $n = 39$) vs. IMP1 high (IHC score ≥ 6, $n = 19$) in our cohort of high-grade glioma (WHO III and GBM) patients. Log-rank $p = 0.0067$. (G) Western blotting analysis to evaluate basal expression of IMP1 in normal human astrocyte (NHA) and well-characterized glioma stem-like cells (GSCs). GAPDH is used as internal control. Quantitative data of the described band are presented below the described band

with short overall survival in GBM (Figure 1C). Consistently, both protein and mRNA levels of IMP1 were observed higher in GBM than in WHO II, III glioma or nontumor tissue (Figure 1D,E) in our cohort of glioma samples. Furthermore, higher IMP1 expression was verified in GBM tumors than in paired adjacent nontumor tissues by Western blotting (Figure S1A). Survival analysis of our cohort of high-grade (WHO III and IV) glioma patients proved that higher IMP1 score (≥6) correlated with worse outcome (Figure 1F). We next tested basal IMP1 protein level in several well-characterized Mes GSCs and PN GSCs,[5,28] and the results showed IMP1 was higher in Mes GSCs than in PN GSCs (Figure 1G, Figure S1B). These results imply that IMP1 is upregulated in high-grade glioma, Mes GBM, and Mes GSCs compared with their counterparts, respectively, correlating with worse outcome in high-grade glioma.

## 3.2 | IMP1 promotes stemness, sphere formation, and tumorigenicity of GSCs

To investigate the physiological role of IMP1, we infected Mes GSCs with two independent short hairpin RNAs of IMP1 (shIMP1) lentiviral vectors. Both the mRNA (Figure 2A) and protein levels (Figure 2B) were well downregulated by shIMP1 in Mes28 and 456. Significant reduction of proliferation rate (Figure 2C) and stem cell

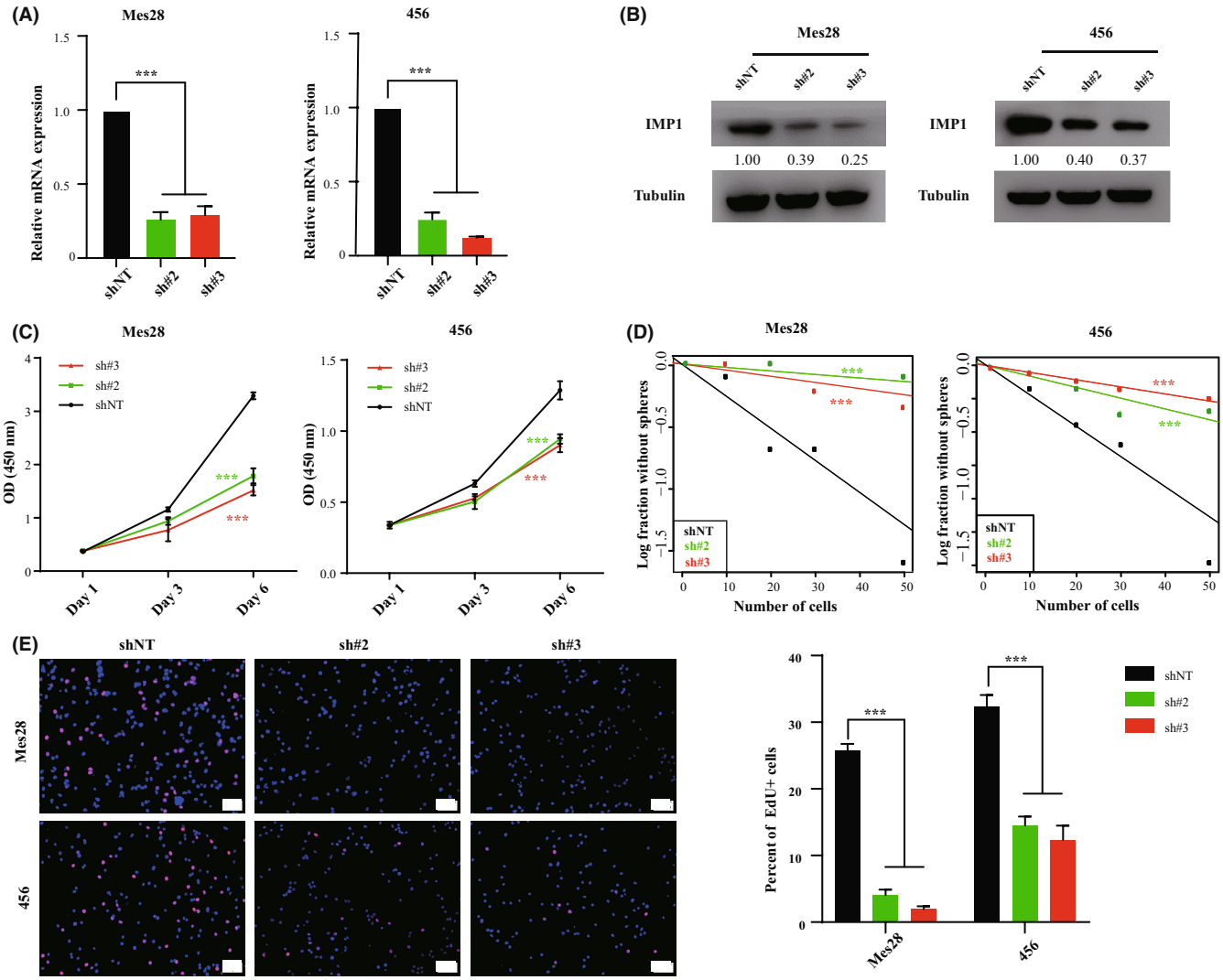


FIGURE 2 Inhibition of IMP1 suppresses proliferation, sphere formation, and stemness of mesenchymal glioblastoma (GBM). (A) RT-PCR analysis for IMP1 in Mes28 and 456 infected with shNT, sh#2, or sh#3 targeting independent regions of the IMP1 lentiviral vectors. $n = 3$ independent experiments; data represent mean ± SD. (B) Western blotting analysis for IMP1 in Mes28 and 456 infected with indicated shIMP1 lentivirus. Tubulin is used as internal control. Quantitative data of the described band are presented below the described band. (C) Proliferation assay of Mes28 and 456 infected with indicated shIMP1 lentivirus. $n = 3$ independent experiments; data represent mean ± SD. (D) Limiting dilution assay of Mes28 and 456 infected with indicated shIMP1 lentivirus after 5-7 d of cell seeding. $n = 3$ independent experiments; data represent mean ± SD. (E) Representative images (left) and histogram (right) of EdU incorporation analysis. Mes28 and 456 infected with indicated shIMP1 lentivirus after 24 h of cell seeding. $n = 3$ independent experiments; data represent mean ± SD

frequency (Figure 2D) were observed in IMP1-silenced Mes GSCs, as well as sphere formation (Figure S2A,B). In addition, the proportion of EdU-incorporated cells was decreased in shIMP1-infected GSCs (Figure 2E).

On the other hand, we sought to validated the above observation by overexpression of IMP1 in PN GSCs. Regarding that the KH3-4 di-domain is indispensable for m6A recognition and binding function of IMP1,[24] wild-type (WT) IMP1, KH1-2 mutants (with the KH3-4 di-domain truncated), and KH3-4 mutants (with the KH1-2 di-domain truncated) were overexpressed in 23 (Figure 3A,B). The proliferation rate and stem cell frequency were increased in WT and KH3-4–overexpressed cells compared with vector and KH1-2 assayed by CCK8 and limited dilution assay, respectively (Figure 3C,D). Sphere formation and EdU incorporation were enhanced by overexpression of IMP1 and KH3-4 mutant (Figure 3E, Figure S2C,D).

We next sought to verify the physiological function of IMP1, in vivo, by intracranial mouse models generated with IMP1-depleted or -overexpressed GSCs. Diminished tumor growth and reduced median survival were observed in mice implanted with shIMP1 GSCs (Figure 4A-D). On the contrary, IMP1 overexpression enhanced in vivo tumor growth and shortened survival of mice (Figure 4E,F). Of note, the wild type of IMP1 showed the most significant impact, followed by KH3-4 mutant, and less effect was also found in KH1-2 mutant (Figure 4E,F). These data indicate that IMP1 is functionally required for GSC property and tumorigenesis, in vivo and in vitro, which depends on the function of m6A recognition and binding.

### 3.3 | IMP1 is required for the mesenchymal signatures of GSCs

Mesenchymal subtype, the most malignant phenotype, is linked to hyperactivation of specific markers and signaling pathways, such as the Hippo pathway.[5,10,16,29] Therefore, we asked if IMP1 impacted mesenchymal signature. IMP1 inhibition markedly attenuated the expression of Mes markers, CD44, YKL40, and VIM,[5,28] in Mes GSCs (Figure 5A), while IMP1 and its mutant resulted in higher expression of CD44, YKL40, and VIM in PN GSC (Figure S3A). Moreover, YAP and its downstream targets (CYR61, ANKRD1, and CTGF) were decreased in IMP1-depleted Mes GSCs (Figure 5B, Figure S3B,D) whereas increased in IMP1-overexpressed PN GSCs (Figure 5C, Figure S3C,E).

Weaker staining of CD44 and YAP and enhanced staining of β-III-tubulin, a neuron-specific marker, were found in xenograft tumors generated from shIMP1-infected 456 cells (Figure 5D and Figure S3F). On the contrary, stronger CD44 and YAP and weaker

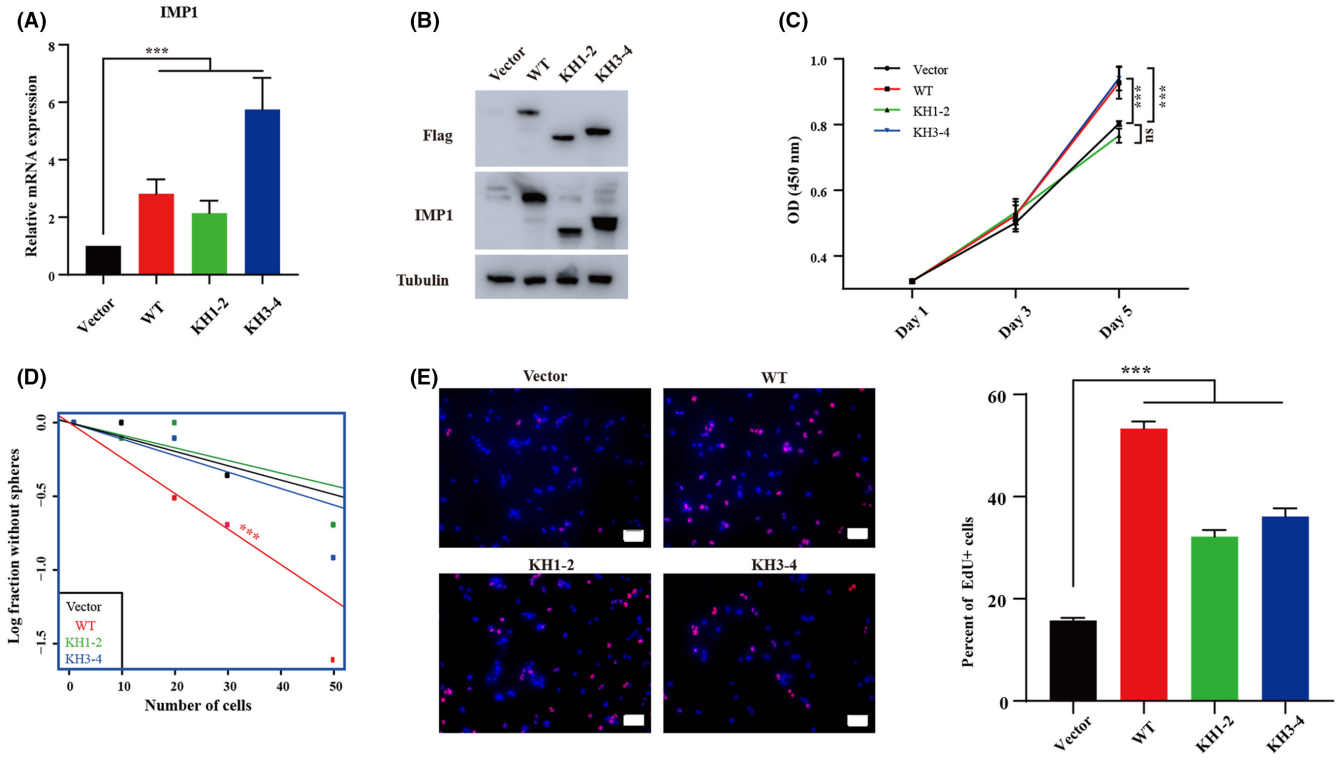


FIGURE 3 Overexpression in IMP1 and its mutant promotes proliferation, sphere formation, and stemness of proneural glioblastoma (GBM). (A) RT-PCR analysis for IMP1 in 23 overexpressed with IMP1 WT, KH1-2 mutant, and KH3-4 mutant. $n = 3$ independent experiments; data represent mean ± SD. (B) Western blotting analysis for IMP1 in 23 overexpressed with indicated form of IMP1. FLAG is used as exogenous tag; tubulin is used as internal control. (C) Proliferation assay of 23 overexpressed with indicated form of IMP1. $n = 3$ independent experiments; data represent mean ± SD. (D) Limiting dilution assay of 23 overexpressed with indicated form of IMP1. $n = 3$ independent experiments; data represent mean ± SD. (E) Representative images (left) and histogram (right) of EdU incorporation analysis in 23 overexpressed with indicated form of IMP1. $n = 3$ independent experiments; data represent mean ± SD

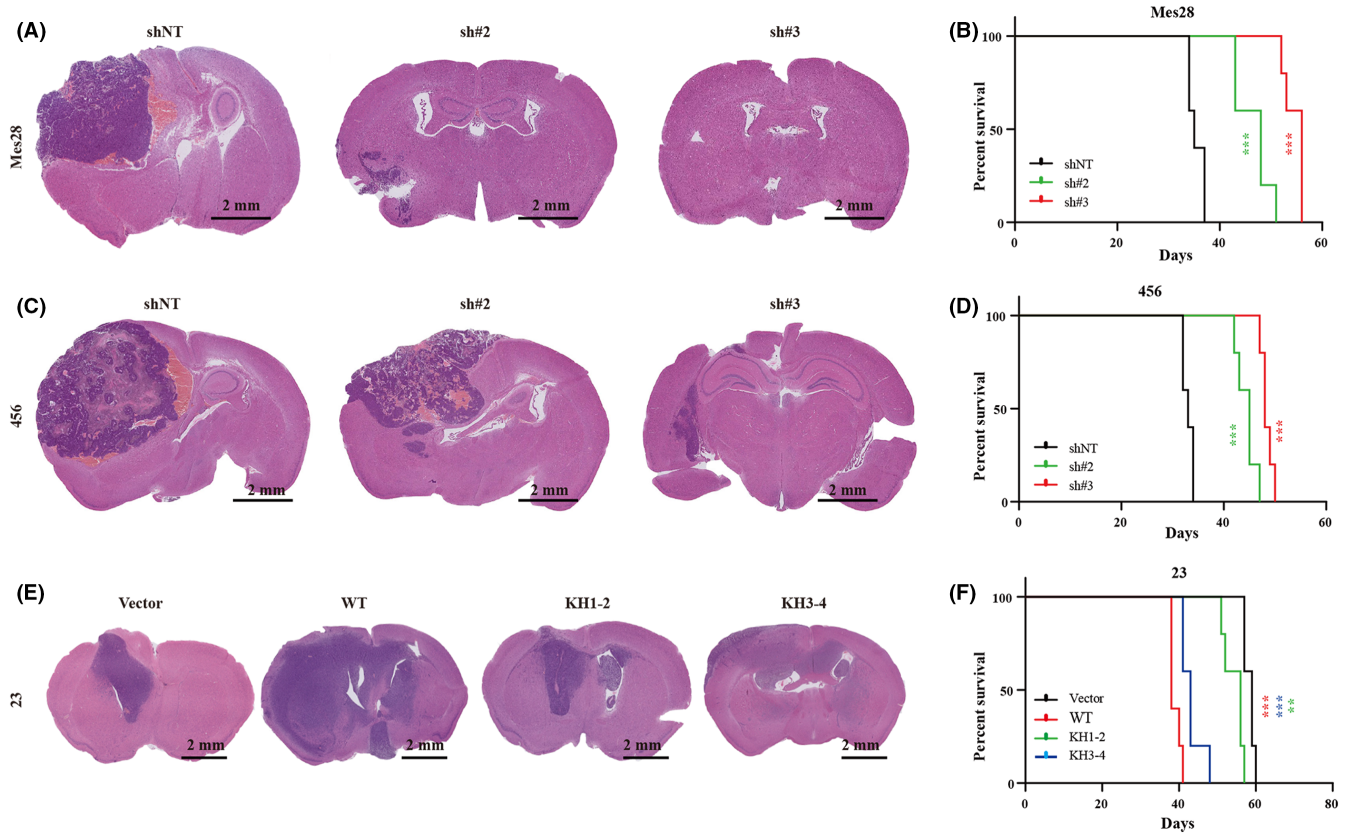


FIGURE 4 IMP1 expression correlates with tumor growth in vivo and mouse survival. (A, C and E) Representative H&E staining of mouse brains harvested on day 32 (Mes28, A) or day 34 (456, C) after implantation of mesenchymal (Mes) glioma stem-like cells (GSCs) expressing shNT, sh#2 or sh#3, and on day 40 (23, E) after implantation of GSCs expressing vector, WT, KH1-2, or KH3-4. Scale bars represent 2 mm. (B, D and F) Kaplan-Meier survival curves of mice intracranially transplanted with Mes28 (B), 456 (D), or 23 (F) GSCs that were infected with indicated lentiviral vectors ($n = 5$)

β-III-tubulin staining were found in xenograft tumors generated from IMP1-overexpressed 23 cells (Figure 5E and Figure S3G). Remarkably, the impact on mesenchymal signatures was significantly attenuated in KH1-2, the KH3-4 di-domain–depleted mutants (Figure 5E, Figure S3A,E,G). Collectively, these results suggest that IMP1 promotes GBM malignant progression, in vitro and in vivo, depending on its m6A recognition and binding function.

### 3.4 | IMP1 activates the Hippo signaling pathway via binding, stabilizing, and enhancing the translation of YAP mRNA

Given the correlation between IMP1 expression and Hippo pathway activation (Figure 5B-E, and Figure S3B-E), we next wanted to explore how IMP1 activates the Hippo signaling pathway. We first treated GSCs with actinomycin D to evaluate YAP mRNA stability. The decay rates of YAP mRNA were higher in IMP1-depleted GSCs and lower in IMP1-overexpressed GSCs (Figure 5F,G), respectively. We next explored if IMP1 binds to YAP mRNA by RNA RIP. Enrichment of YAP and c-Myc (used as positive control) by FLAG RIP was found in WT IMP1– and KH3-4 mutant–overexpressed GSCs (Figure 5H and Figure S4A), suggesting the binding of IMP1 on YAP and c-Myc mRNA. The binding was confirmed by endogenous IMP1 RIP (Figure S4B,C). Furthermore, m$^6$A-meRIP showed that the level of m$^6$A-modified YAP was decreased in shIMP1-infected GSCs and increased in WT IMP1– and KH3-4 mutant–overexpressed GSCs (Figure 5I,J), respectively. Taken together, IMP1 recognizes and binds to m$^6$A-modified YAP mRNA, inducing its stabilization and translation, and thus activates Hippo signaling.

### 3.5 | TAZ functions as an enhancer for IMP1 transcription

Considering the higher expression of IMP1, TAZ, and YAP in high-grade glioma (Figure 1E, Figure S5A,B), we next examined the correlation between IMP1 and YAP/TAZ in human high-grade glioma samples. We detected a moderate correlation between IMP1 and TAZ ($r = 0.4543$, $p < 0.0001$) and weak correlation between IMP1 and YAP ($r = 0.3926$, $p < 0.0001$; Figure 6A,B, and Figure S5C). Previous studies reported a positive feedback loop between IMP1 and c-Myc, in which IMP1 binds to and stabilizes c-Myc mRNA and enhances its translation,[30] while c-Myc transcriptionally regulates IMP1 expression.[31] Also, the transcriptional feedforward loop between YAP and c-Myc was widely studied and well established.[32]

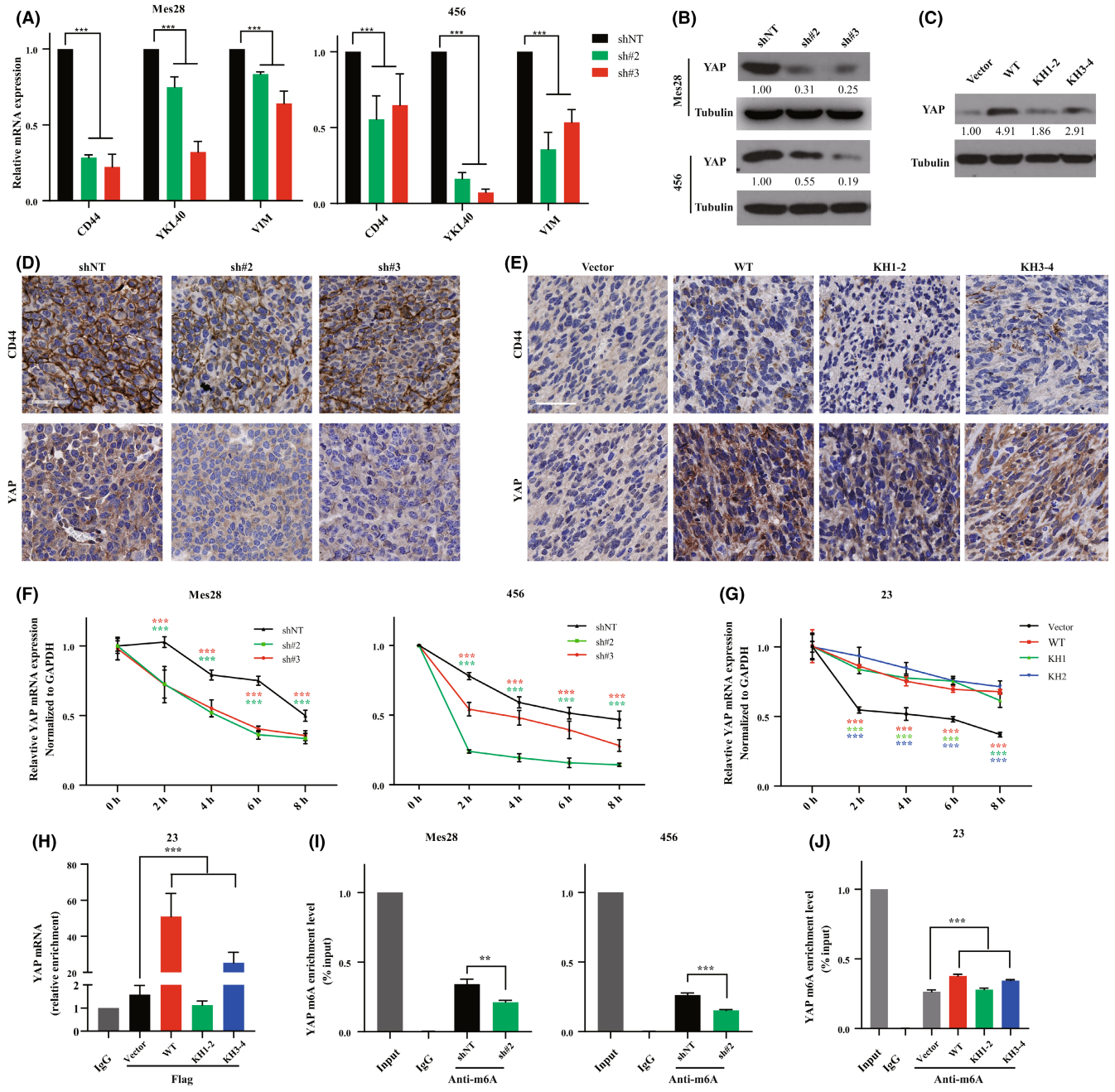


FIGURE 5 IMP1 activates the Hippo signaling pathway via binding, stabilizing, and enhancing translation of YAP mRNA. (A) RT-PCR analysis for mesenchymal markers, CD44, YKL40, and VIM, in Mes28 and 456 infected with shNT-, sh#2-, or sh#3-targeting IMP1 lentiviral vectors. $n = 3$ independent experiments; data represent mean ± SD. (B) Western blotting analysis for YAP in Mes28 and 456 infected with indicated shRNA lentivirus. Tubulin is used as internal control. Quantitative data of the described band are presented below the described band. (C) Western blotting analysis for YAP in 23 overexpressed with indicated form of IMP1. Tubulin is used as internal control. Quantitative data of the described band are presented below the described band. (D) Representative immunohistochemistry (IHC) images for CD44 and YAP in shNT-, sh#2-, or sh#3-infected 456-derived tumors. Scale bar represents 20 μm. (E) Representative IHC images for CD44 and YAP in vector, WT-, KH1-2–, and KH3-4–overexpressed 23-derived tumors. Scale bar represents 20 μm. (F) RT-PCR analysis for YAP mRNA decay rate of Mes28 and 456 infected with shNT, sh#2, or sh#3 virus after actinomycin D treatment for the indicated time. $n = 3$ independent experiments; data represent mean ± SD. (G) RT-PCR analysis for YAP mRNA decay rate of Mes28 and 456 infected with vector, WT, KH1-2, or KH3-4 virus after actinomycin D treatment for the indicated time. $n = 3$ independent experiments; data represent mean ± SD. (H) Histogram of FLAG RNA immunoprecipitation (RIP) coupled with RT-PCR assay for YAP mRNA enrichment in 23 infected with indicated overexpression vectors. $n = 3$ independent experiments; IgG is used as negative control. (I) Histogram of methylated (m6A) RNA immunoprecipitation (MeRIP) coupled with RT-PCR assay for YAP mRNA enrichment in Mes28 and 456 infected with indicated shRNA lentiviral vectors. $n = 3$ independent experiments; IgG is used as negative control. (J) Histogram of methylated (m6A) RNA immunoprecipitation (MeRIP) coupled with RT-PCR assay for YAP $m^6A$ mRNA enrichment in 23 infected with indicated overexpression vectors. $n = 3$ independent experiments; IgG is used as negative control

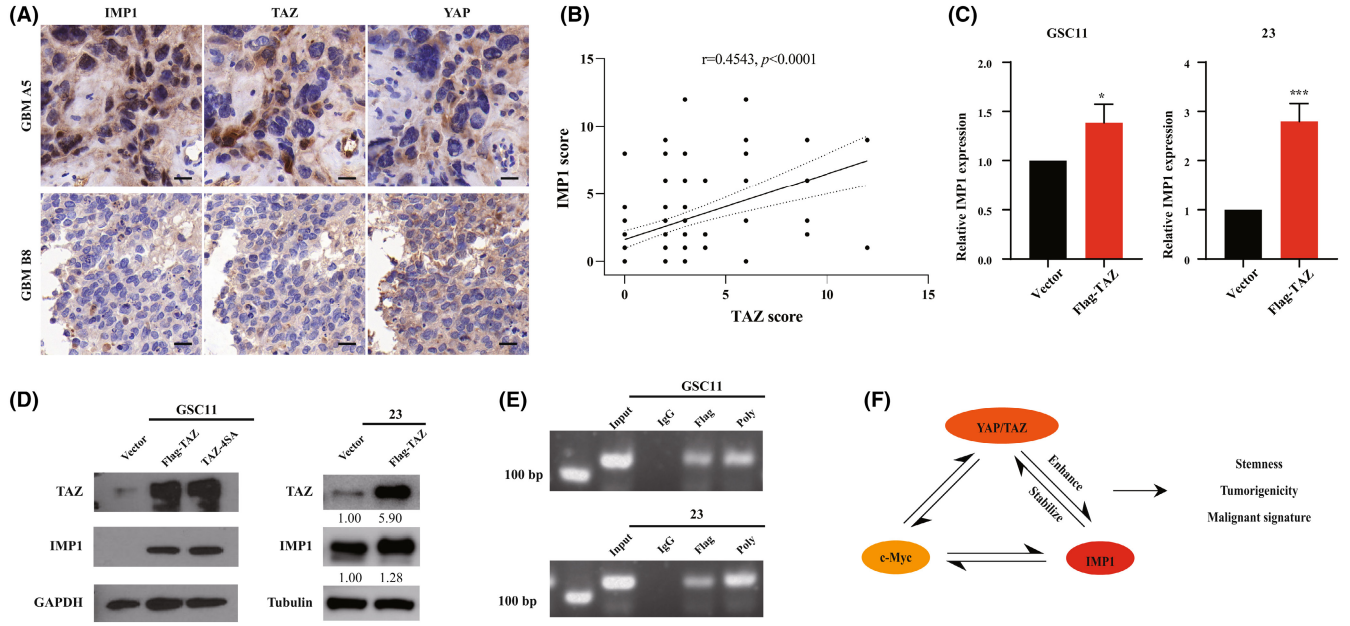


FIGURE 6 TAZ functions as an enhancer for IMP1 transcription. (A) Representative immunohistochemistry (IHC) images for IMP1, TAZ, or YAP in human high-grade glioma samples. Scale bar represents 20 μm. (B) Scatter plot of correlation between expression levels of TAZ and those of IMP1in high-grade glioma samples; $n = 56$, $r = 0.4543$, $p < 0.0001$. (C) RT-PCR analysis of IMP1 expression in vector- and FLAG-TAZ–overexpressed GSC11 and 23. $n = 3$ independent experiments; data represent mean ± SD. (D) Western blotting analysis for TAZ and IMP1 in vector- and FLAG-TAZ–overexpressed GSC11 and 23. GAPDH and tubulin are used as internal control. Quantitative data of the described band are presented below the described band. (E) Northern blotting analysis of enrichment of IMP1 enhancer DNA in vector- and FLAG-TAZ–overexpressed GSC11 and 23. $n = 3$ independent experiments; representative images from one experiment. Poly (polymerase) is used as positive control. (F) Feedforward loop between YAP/TAZ, c-Myc, and IMP1. Related to the present study, YAP/TAZ enhances IMP1 expression, while IMP1 binds to and stabilizes YAP. The feedback loop regulates stemness, tumorigenicity, and mesenchymal-like state of GSCs in glioblastoma (GBM)

These prompted us to check if YAP/TAZ could regulate IMP1 transcription. Considering the stronger correlation between TAZ and IMP1, we overexpressed TAZ in PN GSCs (GSC11 and 23), and verified that TAZ promotes the mRNA and protein levels of IMP1 (Figure 6C,D). Zanconato et al.[33] revealed that more than 90% of YAP/TAZ-bound elements correspond to enhancer elements for transcriptional regulation. ChIP-PCR verified TAZ binding to the enhancer of IMP1 (Figure 6E), confirming the binding of YAP/TAZ to the distant enhancer element of IMP1.[33] These data reveal that YAP/TAZ function as enhancer of IMP1 expression.

## 4 | DISCUSSION

Intratumoral heterogeneity and plasticity in GBM are considered to be the main causes for tumor progression and therapeutic resistance.[7,34,35] The present study suggests a feedback loop between IMP1 and YAP/TAZ signaling regulating GSC characteristics, tumorigenicity, and malignant progression in GBM.

We firstly demonstrate that IMP1 is upregulated in mesenchymal GBM and GSCs, and its higher expression correlates with short patient survival. Overexpression of IMP1 in PN GSC promotes while IMP1 knockdown in Mes GSCs attenuates tumorigenesis and malignant progression. Noteworthily, both WT KH3-4 and mutant KH3-4 show comparable physiological effect; however, KH1-2 mutant shows less impact. This evidence suggests that the physiological function of IMP1 largely depends on its $m^6A$ recognition and binding function (Figure 3-5, Figures S2 and S3). We confirm that IMP1 mechanically binds to $m^6A$-modified YAP mRNA, enhancing its translation, and hence induces Hippo pathway activation (Figure 5, Figures S3 and S4).

Except the binding and stabilization of IMP1 to YAP, we also prove TAZ functions as enhancer of IMP1, suggesting a feedforward loop between YAP/TAZ and IMP1. In the literature, positive feedback loops between IMP1 and c-Myc[30,31] and between YAP and c-Myc[32] are well established. Therefore, our data and previous reports strongly suggest a feedback loop between IMP1, c-Myc, and YAP/TAZ (Figure 6F). Mahapatra and colleagues identified the first IMP1 inhibitor, BTYNB, which could inhibit IMP1 binding to a specific high-affinity binding site of target mRNA, including c-Myc, β-TrCP1, and E2F.[36,37] In the present study, BTYNB also inhibits the binding of IMP1 to YAP mRNA and hence suppresses YAP activation in GSCs (Figure S5D-F). The antitumor efficacy of BTYNB was verified in a mouse model in an IMP1-dependent way.[37] With the new first-in-class c-Myc inhibitor being put into clinical assessment in 2021,[38] the combinational strategy targeting the IMP1-c-Myc-YAP/TAZ feedback loop in cancer including GBM seems prospective; however, it needs further investigation.

In conclusion, this study elicits a critical role of the IMP1-YAP/TAZ feedback loop in tumorigenesis and malignant progression and

suggests IMP1 as an attractive target for the treatment of aggressive GBM. Also, our findings reveal a nontranscriptional regulation of YAP/TAZ signaling in GBM. Given the characteristics of a feedforward loop between IMP1, YAP/TAZ, and c-Myc, our data also provide a potential therapeutic intervention of combinational inhibition in GBM treatment.

## ACKNOWLEDGEMENT

We appreciate the kind gift from Dr. Yunfei Yuan and Dr. Yunxing Shi, members of the department of Hepatobilliary Oncology, Cancer Center, Sun Yat-sen University, Guangzhou, China. And we thank Dr. Xinya Gao, member of the Department of Neurosurgery, the First Affiliated Hospital of Sun Yat-sen University, Guangzhou, China.

## DISCLOSURE

The authors declare that the work described is original work and is not under review by any other journal. There is no conflict of interest in the submission of this manuscript.

## DATA AVAILABILITY STATEMENT

There is no new data generated or analyzed in the present study. All RNA sequence or microarray data were download from GlioVis brain tumor dataset or GEO dataset with indicated accession number in the manuscript. Please contact Dr. Deng for any materials used in the study.

## CONSENT FOR PUBLICATION

All the authors have read the final version of this manuscript and approved it for publication.

## ETHICS STATEMENT

The authors declare that the study was approved and conducted in accordance with the policies of the Scientific Ethics Committee of the First Affiliated Hospital of Sun Yat-sen University and the First Affiliated Hospital of Xi'an Jiaotong University. All human tissues were collected with written informed consent. The approval number of the study is [2021]-172. All animal procedures were reviewed and approved by the Institutional Animal Care and Use Committee (IACUC) at Sun Yat-sen University in accordance with NIH and institutional guidelines, conforming to the provisions of the Declaration of Helsinki.

## ORCID

*Jia Yang* https://orcid.org/0000-0002-6265-0864
*Xujia Wu* https://orcid.org/0000-0002-6904-0778
*Jia Wang* https://orcid.org/0000-0002-4746-035X
*Zhong Deng* https://orcid.org/0000-0002-3510-1376

## REFERENCES

1. Ostrom QT, Patil N, Cioffi G, Waite K, Kruchko C, Barnholtz-Sloan JS. CBTRUS statistical report: primary brain and other central nervous system tumors diagnosed in the United States in 2013-2017. *Neuro Oncol*. 2020;22:iv1-iv96.
2. Wang Q, Hu B, Hu X, et al. Tumor evolution of glioma-intrinsic gene expression subtypes associates with immunological changes in the microenvironment. *Cancer Cell*. 2017;32:42-56.e46.
3. Verhaak RG, Hoadley KA, Purdom E, et al. Integrated genomic analysis identifies clinically relevant subtypes of glioblastoma characterized by abnormalities in PDGFRA, IDH1, EGFR, and NF1. *Cancer Cell*. 2010;17:98-110.
4. Phillips HS, Kharbanda S, Chen R, et al. Molecular subclasses of high-grade glioma predict prognosis, delineate a pattern of disease progression, and resemble stages in neurogenesis. *Cancer Cell*. 2006;9:157-173.
5. Bhat KPL, Balasubramaniyan V, Vaillant B, et al. Mesenchymal differentiation mediated by NF-κB promotes radiation resistance in glioblastoma. *Cancer Cell*. 2013;24:331-346.
6. Patel AP, Tirosh I, Trombetta JJ, et al. Single-cell RNA-seq highlights intratumoral heterogeneity in primary glioblastoma. *Science*. 2014;344:1396-1401.
7. Hara T, Chanoch-Myers R, Mathewson ND, et al. Interactions between cancer cells and immune cells drive transitions to mesenchymal-like states in glioblastoma. *Cancer Cell*. 2021;39:779-792.e711.
8. Halliday J, Helmy K, Pattwell SS, et al. In vivo radiation response of proneural glioma characterized by protective p53 transcriptional program and proneural-mesenchymal shift. *Proc Natl Acad Sci USA*. 2014;111:5248-5253.
9. Mao P, Joshi K, Li J, et al. Mesenchymal glioma stem cells are maintained by activated glycolytic metabolism involving aldehyde dehydrogenase 1A3. *Proc Natl Acad Sci U S A*. 2013;110:8644-8649.
10. Minata M, Audia A, Shi J, et al. Phenotypic plasticity of invasive edge glioma stem-like cells in response to ionizing radiation. *Cell Rep*. 2019;26:1893-1905.e1897.
11. Lu KV, Chang JP, Parachoniak CA, et al. VEGF inhibits tumor cell invasion and mesenchymal transition through a MET/VEGFR2 complex. *Cancer Cell*. 2012;22:21-35.
12. Mathew LK, Skuli N, Mucaj V, et al. miR-218 opposes a critical RTK-HIF pathway in mesenchymal glioblastoma. *Proc Natl Acad Sci USA*. 2014;111:291-296.
13. Zanconato F, Cordenonsi M, Piccolo S. YAP/TAZ at the roots of cancer. *Cancer Cell*. 2016;29:783-803.
14. Sanchez-Vega F, Mina M, Armenia J, et al. Oncogenic signaling pathways in the cancer genome atlas. *Cell*. 2018;173:321-337.e310.
15. Dey A, Varelas X, Guan KL. Targeting the hippo pathway in cancer, fibrosis, wound healing and regenerative medicine. *Nat Rev Drug Discov*. 2020;19:480-494.
16. Bhat KP, Salazar KL, Balasubramaniyan V, et al. The transcriptional coactivator TAZ regulates mesenchymal differentiation in malignant glioma. *Genes Dev*. 2011;25:2594-2609.
17. Orr BA, Bai H, Odia Y, Jain D, Anders RA, Eberhart CG. Yes-associated protein 1 is widely expressed in human brain tumors and promotes glioblastoma growth. *J Neuropathol Exp Neurol*. 2011;70:568-577.
18. Basu-Roy U, Bayin NS, Rattanakorn K, et al. Sox2 antagonizes the hippo pathway to maintain stemness in cancer cells. *Nat Commun*. 2015;6:6411.
19. Zhang Y, Wang Y, Zhou D, et al. Radiation-induced YAP activation confers glioma radioresistance via promoting FGF2 transcription and DNA damage repair. *Oncogene*. 2021;40:4580-4591.
20. Cosset É, Ilmjärv S, Dutoit V, et al. Glut3 addiction is a druggable vulnerability for a molecularly defined subpopulation of glioblastoma. *Cancer Cell*. 2017;32:856-868.e855.
21. Carro MS, Lim WK, Alvarez MJ, et al. The transcriptional network for mesenchymal transformation of brain tumours. *Nature*. 2010;463:318-325.
22. Vigneswaran K, Boyd NH, Oh SY, et al. YAP/TAZ transcriptional coactivators create therapeutic vulnerability to verteporfin in EGFR-mutant glioblastoma. *Clin Cancer Res*. 2021;27:1553-1569.

23. Nielsen J, Christiansen J, Lykke-Andersen J, Johnsen AH, Wewer UM, Nielsen FC. A family of insulin-like growth factor II mRNA-binding proteins represses translation in late development. *Mol Cell Biol*. 1999;19:1262-1270.
24. Huang H, Weng H, Sun W, et al. Recognition of RNA N(6)-methyladenosine by IGF2BP proteins enhances mRNA stability and translation. *Nat Cell Biol*. 2018;20:285-295.
25. Degrauwe N, Suvà ML, Janiszewska M, Riggi N, Stamenkovic I. IMPs: an RNA-binding protein family that provides a link between stem cell maintenance in normal development and cancer. *Genes Dev*. 2016;30:2459-2474.
26. Hanniford D, Ulloa-Morales A, Karz A, et al. Epigenetic silencing of CDR1as drives IGF2BP3-mediated melanoma invasion and metastasis. *Cancer Cell*. 2020;37:55-70.e15.
27. Martindale JL, Gorospe M, Idda ML. Ribonucleoprotein immunoprecipitation (RIP) analysis. *Bio Protoc*. 2020;10:e3488.
28. Jin X, Kim LJY, Wu Q, et al. Targeting glioma stem cells through combined BMI1 and EZH2 inhibition. *Nat Med*. 2017;23:1352-1361.
29. Liao Y, Luo Z, Deng Y, et al. OLIG2 maintenance is not essential for diffuse intrinsic pontine glioma cell line growth but regulates tumor phenotypes. *Neuro Oncol*. 2021;23:1183-1196.
30. Noubissi FK, Elcheva I, Bhatia N, et al. CRD-BP mediates stabilization of betaTrCP1 and c-myc mRNA in response to beta-catenin signalling. *Nature*. 2006;441:898-901.
31. Noubissi FK, Nikiforov MA, Colburn N, Spiegelman VS. Transcriptional regulation of CRD-BP by c-myc: implications for c-myc functions. *Genes Cancer*. 2010;1:1074-1082.
32. Neto-Silva RM, de Beco S, Johnston LA. Evidence for a growth-stabilizing regulatory feedback mechanism between Myc and Yorkie, the drosophila homolog of yap. *Dev Cell*. 2010;19:507-520.
33. Zanconato F, Forcato M, Battilana G, et al. Genome-wide association between YAP/TAZ/TEAD and AP-1 at enhancers drives oncogenic growth. *Nat Cell Biol*. 2015;17:1218-1227.
34. Brennan CW, Verhaak RG, McKenna A, et al. The somatic genomic landscape of glioblastoma. *Cell*. 2013;155:462-477.
35. Neftel C, Laffy J, Filbin MG, et al. An integrative model of cellular states, plasticity, and genetics for glioblastoma. *Cell*. 2019;178:835-849.e821.
36. Mahapatra L, Andruska N, Mao C, Le J, Shapiro DJ. A novel IMP1 inhibitor, BTYNB, targets c-Myc and inhibits melanoma and ovarian cancer cell proliferation. *Transl Oncol*. 2017;10:818-827.
37. Müller S, Bley N, Busch B, et al. The oncofetal RNA-binding protein IGF2BP1 is a druggable, post-transcriptional super-enhancer of E2F-driven gene expression in cancer. *Nucleic Acids Res*. 2020;48:8576-8590.
38. Whitfield JR, Soucek L. The long journey to bring a Myc inhibitor to the clinic. *J Cell Biol*. 2021;220:e202103090.


## SUPPORTING INFORMATION

Additional supporting information can be found online in the Supporting Information section at the end of this article.

**How to cite this article:** Yang J, Wu X, Wang J, et al. Feedforward loop between IMP1 and YAP/TAZ promotes tumorigenesis and malignant progression in glioblastoma. *Cancer Sci*. 2023;114:2053-2062. doi: 10.1111/cas.15636